Available online at www.sciencedirect.com
SCIENCE DIRECT
Journal of Power Sources 156 (2006) 23–27
JOURNAL OF POWER SOURCES
www.elsevier.com/locate/jpowsour

Short communication

Protective coating for MCFC cathode: Low temperature potentiostatic deposition of CoOOH on nickel in aqueous media containing glycine

C. Mansour, T. Pauporté, A. Ringuedé, V. Albin, M. Cassir *

Laboratoire d'Electrochimie et de Chimie Analytique, ENSCP, UMR 7575 CNRS, 11 rue Pierre et Marie Curie, 75231 Paris Cedex 05, France

Available online 8 November 2005

Abstract

The corrosion and dissolution of the state-of-the-art nickel cathode is one of the major problems for the development of the molten carbonate fuel cell. In order to protect this cathode, electrochemical potentiostatic deposition, a cheap and low-temperature technique, was used to produce CoOOH coating. It is well known that the lithiated cobalt oxide ($LiCoO_2$, stable from produced at 650 °C in molten carbonates) is significantly less soluble than nickel oxide. Potential–acidity diagrams of the cobalt–water system with the presence of a complexing agent, glycine, established from a new critical data set, allowed to predict the thermodynamic stability of CoOOH in a range of 25–80 °C. The deposition process was optimised on dense nickel substrates, analysing thoroughly the effect of the temperature, imposed potential, pH, electrolysis duration and the role of glycine. The structure and morphology of the thin layers prepared were characterised by X-ray diffraction and scanning electron microscopy (SEM). XRD measurements showed the presence of the characteristic CoOOH lines in varied experimental conditions. The CoOOH coatings were spontaneously transformed into $LiCoO_2$ in the molten carbonate melt. Preliminary results, obtained from ex situ and in situ techniques, on their behaviour and stability in MCFC conditions are given here.

Keywords: Cobalt oxides; Electrodeposition; Glycine; Fuel cells; MCFC cathode coating

1. Introduction

The cathode usually used in molten carbonate fuel cell (MCFC) is a nickel electrode covered by nickel oxide NiO. In the functional MCFC conditions (650 °C, air/CO_2 70:30 (mol%)), this cathode can be easily dissociated (by chemical dissolution) which limits the development of these fuel cells. Thermodynamic studies allow to predict the dissolution of NiO into Ni^{2+} in Li_2CO_3–Na_2CO_3–K_2CO_3 or Li_2CO_3–K_2CO_3 eutectic usually used as MCFC electrolytes [1,2]. It is well known that lithium cobaltite, $LiCoO_2$, is significantly less soluble than nickel oxide. In order to combine the conductive and electrocatalytic properties of the nickel cathode with the protective role of $LiCoO_2$ [3–5], it is proposed to cover the surface of the nickel electrode by a film of cobalt oxide (Co_3O_4 or CoOOH). Lithium cobaltite is the stable form of cobalt at high temperature, then, the formed oxide is transformed into $LiCoO_2$ at 650 °C. Cobalt oxide coatings were produced by electrochemical potentiostatic deposition, a cheap and low temperature technique, thoroughly described in previous studies in the case of the oxidation of a $Co(OH)_2$ suspension on nickel dense or porous substrates [6–10]. In the present study, cobalt oxide is deposited on a dense nickel substrate, oxidising Co(II) in an aqueous solution containing glycine (NH_2CH_2COOH); the role of this complexing agent here is to stabilise the soluble form of Co(II) at lower acidity levels favourable to the oxidation process. To predict the behaviour of cobalt species in this medium, Potential–acidity diagrams of the cobalt–water system with the presence of glycine are plotted, using new critical data set [11,12], in a range of 25–80 °C. The films of cobalt oxide are deposited on dense nickel substrates after analysing the effect of the temperature, imposed potential, pH, electrolysis duration and the role of glycine. Deposition conditions were fixed after hydrodynamical voltammetry and electrochemical quartz crystal microbalance studies. Nickel electrodes protected by cobalt oxide films were immersed in molten carbonate bulk (with MCFC operating conditions), the behaviour of the protected electrode in the bulk is followed in situ by chronopotentiometry without dc current (open circuit potential, OCP). The structure and morphology of the thin layers prepared were characterised by X-ray diffraction and scanning electron microscopy (SEM) before and after immersion in molten carbonate bulk and solubility measurements of

* Corresponding author. Tel.: +33 1 55426387; fax: +33 1 44276750.
E-mail address: michel-cassir@enscp.fr (M. Cassir).

0378-7753/$ – see front matter © 2005 Elsevier B.V. All rights reserved.
doi:10.1016/j.jpowsour.2005.08.020

nickel were analysed by Inductively Coupled Plasma Atomic Emission Spectroscopy (ICP-AES).

2. Experimental procedure

2.1. Thermodynamic predictions

Equilibrium diagrams of cobalt–water–glycine systems were established, using new critical data set [13]. These diagrams were plotted at different temperatures (25, 40, 60 and 80 °C) in order to predict the effect of this parameter on the stability of cobalt species.

Fig. 1 shows the Potential–acidity diagram at 25 and 80 °C. It can be noted that both Co_3O_4 and CoOOH species can be stabilised. In our experimental conditions (*E*, pH), as will be seen further on, CoOOH is the stable form obtained by Co(II) oxidation. When the temperature increases, the stability domain of CoOOH tends to be reduced with respect to Co_3O_4 one, nevertheless it is still CoOOH which is formed by Co(II) oxidation at 80 °C. XRD analysis confirms that the elaborated films are CoOOH coatings.

The free energy of formation $\Delta_f G_{CoOOH} = -94.25$ kcal mol^{-1} selected in this work to plot the potential–acidity diagrams is the intermediate value between a correlated value, −96.22 kcal mol^{-1} (deduced from $\Delta_f H$ and S° values of FeOOH and NiOOH), and an experimental one, −92.3 kcal mol^{-1} [11]. The cobalt and glycine concentrations used to plot *E*–pH diagrams are the same than those used to produce protective coatings by electrochemical deposition, and the complexing agent $NH_2CH_2COO^-$ is replaced by L.

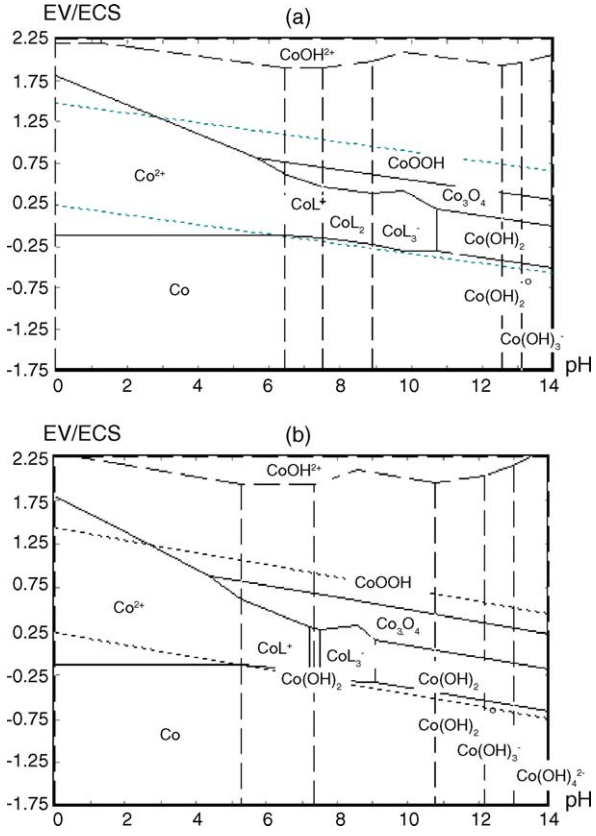

Fig. 1. Potential–acidity diagrams of cobalt–water system with presence of glycine, $[Co^{2+}] = 2 \times 10^{-3}$ mol L^{-1}, $[NH_2CH_2COOH] = 2 \times 10^{-2}$ mol L^{-1}. (a) $T = 25$ °C and (b) $T = 80$ °C.

2.2. Hydrodynamic voltammetric analysis

Acidity levels and temperature effects were analysed using this electrochemical technique.

The solution is a mixture of 0.002 mol L^{-1} $Co(NO_3)_2{\cdot}6H_2O$ and 0.5 mol L^{-1} $NaNO_3$. The counter electrode is a platinum wire, the reference electrode is a saturated calomel electrode (SCE) and the working electrode is a rotating nickel disk electrode which allows the establishment of the hydrodynamic regime.

First, the pH effect was studied with a temperature fixed at 25 °C and then *I–E* curves were recorded at different pH (8.5, 9.5, 10.5 and 11.5) by hydrodynamic voltammetry, the potential sweep varying from 0 to 1.5 V/SCE.

The temperature effect was studied, with a pH value fixed at 10.5 and *I–E* curves were recorded by varying the temperature in a range of 25–80 °C (25, 40, 60 and 80 °C).

2.3. Electrochemical quartz crystal microbalance analysis

The mass uptake was followed in situ with an electrochemical quartz crystal microbalance set up. The previous experimental cell was used in the same conditions, quartz single crystals were covered by gold thin film electrodes on both faces, one of the gold electrodes was exposed to the electrolyte and used as the working electrode for deposition. During the deposition, the current density was simultaneously recorded and the exchanged charge was obtained by integrating the current density versus time curve.

To study the potential effect, temperature was fixed at 80 °C and thin films were deposited on the quartz electrode at different potentials (0.75, 0.8 and 0.9 V/SCE) during 40 min. Then, the potential was fixed at 0.8 V/SCE and cobalt oxide films were deposited at different temperatures (25, 40, 60 and 80 °C).

2.4. Elaboration of cobalt oxide coatings

Elaboration conditions of the cobalt oxide coatings were fixed after studying the temperature, pH and potential effects by the means of hydrodynamic voltammetry and electrochemical quartz microbalance analysis. Four films of cobalt oxide were elaborated on nickel plates (their surface being 1 cm^2) in the same experimental conditions than the hydrodynamic voltammetry. Cobalt oxide was deposited on both faces of the working electrode (2 cm^2) by potentiostatic electrolysis, the deposition time being 8 h and the pH fixed at 10.5. Elaboration conditions are described below:

- $T = 25$ °C, $E = 0.8$ V/SCE
- $T = 25$ °C, $E = 0.85$ V/SCE

- $T = 80\,^{\circ}C$, $E = 0.8$ V/SCE
- $T = 80\,^{\circ}C$, $E = 0.85$ V/SCE

The thin films elaborated were characterised by scanning electron microscopy (SEM) and surface analysis.

2.5. Electrochemical performance in molten carbonate

In order to study the performance of the elaborated films, operating MCFC conditions were applied. The Ni plates covered by cobalt oxide coatings were used as working electrodes in a cell containing the Li_2CO_3–Na_2CO_3 eutectic. The temperature was fixed at 650 °C in a mixture of air/CO_2 70:30 (mol%). The reference electrode is a silver wire in contact with the eutectic saturated with Ag_2SO_4, so the reference system is Ag^+/Ag. The counter electrode is a gold wire, extra pure (99.9%).

The behaviour of the nickel plates in these conditions was followed in situ by open circuit potential (OCP) for 48 h. Then the nickel electrodes were characterised by SEM with surface analysis and ICP/AES measurements.

3. Results and discussion

Fig. 2 shows the effect of the temperature and the pH on the hydrodynamic voltammetric curves. The first anodic wave observed shifts towards more negative potential with increasing the electrolyte temperature or the pH (in agreement with the thermodynamic diagrams showing a similar shift). The current

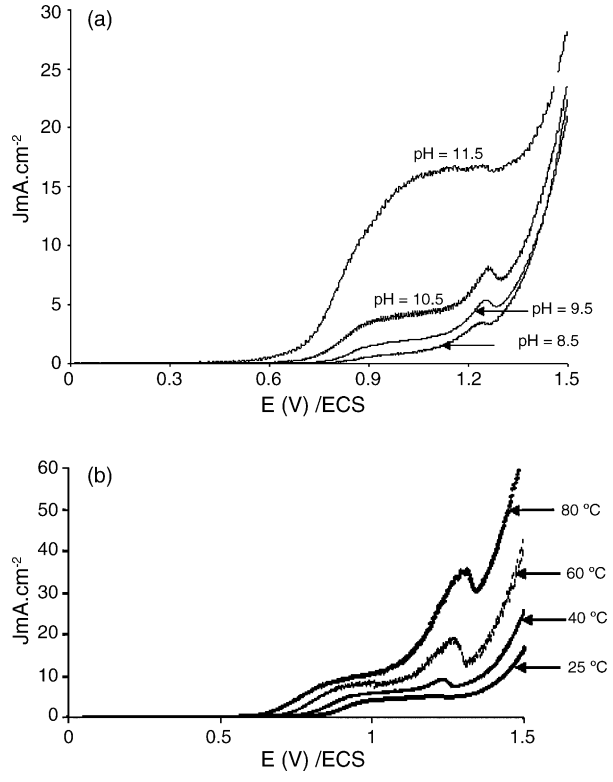

Fig. 2. Steady state *I–E* curves in a 2×10^{-3} mol L^{-1} [Co^{2+}], [NH_2CH_2COOH] at 2×10^{-2} mol L^{-1}. (a) pH effect at $T = 25\,^{\circ}C$ and (b) temperature effect at pH 10.5.

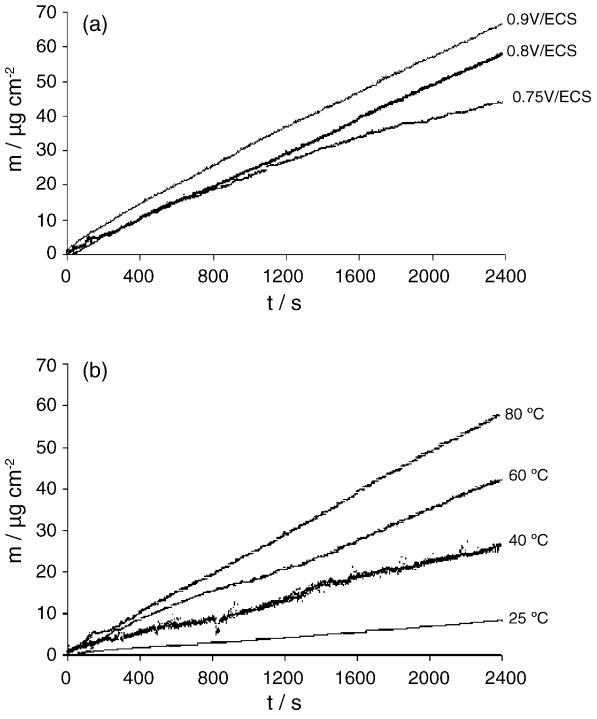

Fig. 3. Electrochemical quartz crystal microbalance measurements, variation of the mass uptake vs. time. (a) Potential effect at $T = 25\,^{\circ}C$ and (b) temperature effect at $E = 0.8$ V/SCE.

also increases with the temperature, which means that the reaction kinetics increases with the temperature. This anodic wave corresponds to the oxidation of Co(II) into CoOOH or Co_3O_4. The peak following the oxidation waves increases with the pH and with the temperature. When the used glycine is not electroactive, the peak cannot be related to the adsorption of glycine on the working electrode but it can be due to the adsorption of a complex cobalt–glycine.

The mass uptake was followed by the electrochemical quartz crystal microbalance technique at different potentials and temperatures (Fig. 3). The film growth rate increases linearly with the potential and the electrolyte temperature. It can be noted that the thin films formed on the surface of the gold electrode at high potential are easily dissolved, which means that the adherence of the deposited films decreases by increasing the potential. Using the mass deposited, film thicknesses are calculated and reported in Table 1. Even though the mass deposited reaches 87 µg cm^{-2} h^{-1}, it is low in comparison with the mass deposited without glycine which can reach 146 µg cm^{-2} h^{-1} [13]. This means that glycine, at least with the considered concentration

Table 1
Variation of the deposition rate and films thicknesses with the temperature

Temperature (°C)	Deposited mass (µg cm^{-2} h^{-1})	Thickness of deposited film (µm h^{-1})
25	12	0.015
40	39	0.06
60	63	0.12
80	87	0.16

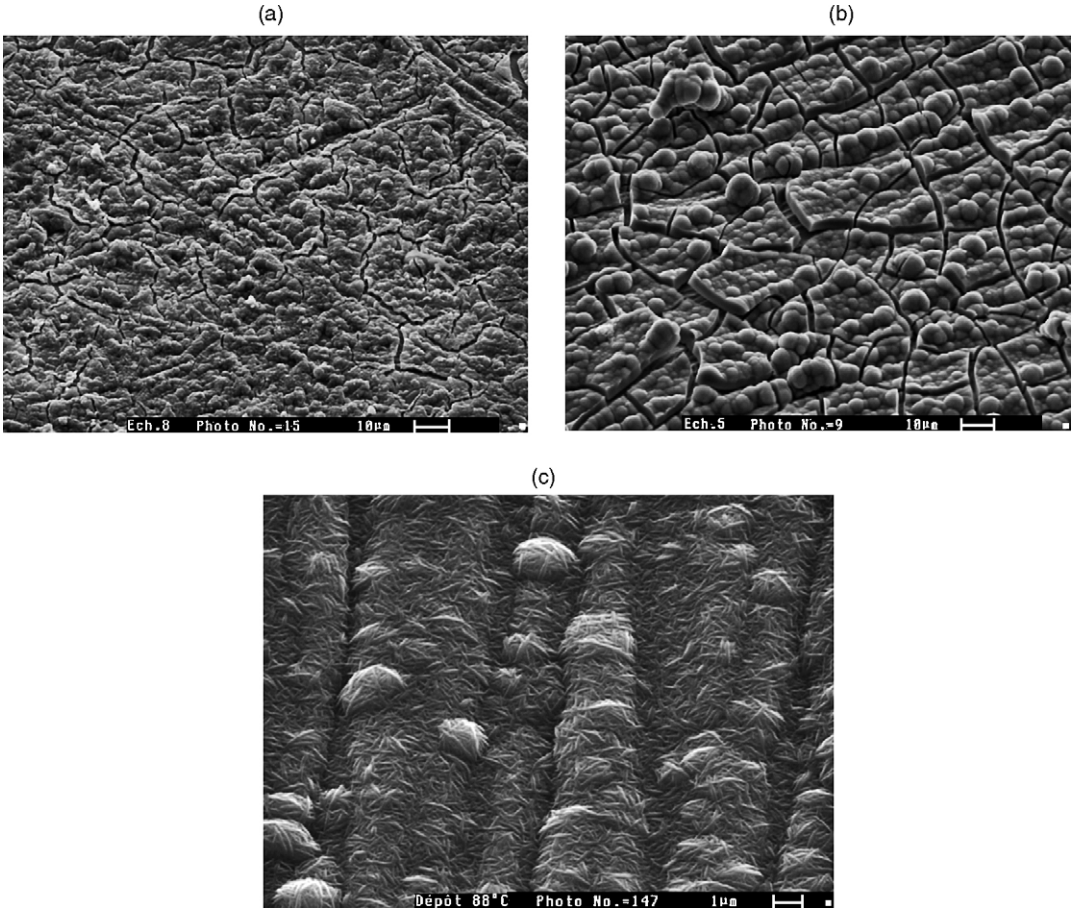

Fig. 4. SEM micrographs of films deposited at 25 and 80 °C: (a) 25 °C in presence of glycine, (b) 80 °C in presence of glycine and (c) 80 °C without glycine.

has, a negative effect on the yield of the electrochemical deposition reaction.

Fig. 4 shows SEM characterisation of coatings at 25 and 80 °C. The films are not well covering and their adherence decreases when increasing the temperature, and at 80 °C they are not crystallized. They are less adherent than films produced without glycine, which can be due to an adsorption of glycine at the surface of the plate. Surface analysis, reported in Table 2, shows that Ni is completely oxidised into NiO and that at 80 °C CoOOH is the species formed. It shows also that the thickness of the films increases with the temperature and the potential.

OCP curves for all the films have a similar aspect. In Fig. 5, an example is given on cobalt oxide-coated Ni at 25 °C. The initial potential corresponds to Ni/NiO system [13,14], then the potential increases due to the formation of a NiO layer which evolves with the time; afterwards, the lithiation phenomenon takes place with the incorporation of Li^+ in the NiO/Co_3O_4 film. Then lithi-

Table 2
Surface analysis: variation of the film thickness with the temperature and the imposed potential

Temperature (°C)	Co (at.%)	Ni (at.%)	O (at.%)	Thickness (μm)
Influence of the temperature at $E = 0.80$ V/ECS				
25	11	31	58	0.6
80	29	8	63	2.0
E (V/ECS)	Co (at.%)	Ni (at.%)	O (at.%)	Thickness (μm)
Influence of the imposed potential at 25 °C				
0.80	11	31	58	0.6
0.85	12	25	63	1.0
Influence of the imposed potential at 80 °C				
0.75	9	32	59	0.4
0.8	29	8	63	2.0

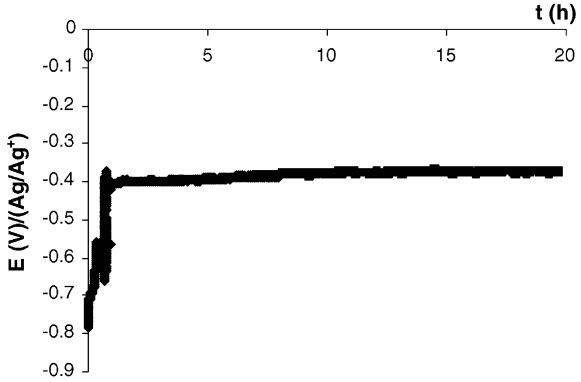

Fig. 5. OCP measurements obtained on cobalt oxide-coated nickel electrode with the presence of glycine ($[NH_2CH_2COOH]$ at 2×10^{-2} mol L^{-1}) at 25 °C.

Table 3
Surface analysis and ICP measurements after immersion in the molten carbonate

Sample	EDS after immersion			ICP after immersion	
	Co (at.%)	Ni (at.%)	O (at.%)	[Co] × 10^5 (mol kg^{-1})	[Ni] × 10^5 (mol kg^{-1})
25 °C with glycine (22 h of immersion)	3	45	52	2 (or 10 ppb)	9
80 °C with glycine (6 h of immersion)	2	46	52	2	10
80 °C without glycine (48 h of immersion)	3	45	52	2	7

ated oxides are formed, such as $LiCoO_2$ and $Li_x^+Ni_x^{3+}Ni_{1-2x}^{2+}O^{2-}$ [14,15], corresponding to the reactions below:

$$(1-x)NiO + \frac{x}{2}Li_2CO_3 + \frac{x}{4}O_2 \rightarrow Li_x^+Ni_x^{3+}Ni_{1-2x}^{2+}O^{2-} + \frac{x}{2}CO_2$$

$$Co_3O_4 + 3Li^+ + 2CO_3^{2-} \rightarrow 3LiCoO_2 + 2CO_2 + e^-$$

Afterwards, the potential increases reaching a relatively stable value of −0.4 V/Ag^+/Ag, corresponding to the equilibrium potential of an oxidised and lithiated metallic non-coated nickel electrode [13].

ICP measurements, reported in Table 3, show that nickel electrode coated by cobalt oxide is less soluble than a non-protected electrode. It shows also that the cobalt is not soluble comparing to nickel, it can be noted that after operating in MCFC bath, a little proportion of cobalt is left on nickel plate surface; in fact, the loss of the film is due to a mechanical drop of the cobalt oxide. Even though, it can be supposed that some cobalt had diffused to the plate and formed with the nickel a mixed oxide $LiNi_{1-x}Co_xO_2$ [16–18].

4. Conclusion

In agreement with thermodynamic predictions, hydrodynamic voltammetric analysis and electrochemical quartz crystal microbalance analysis, conditions were fixed to elaborate thin films of cobalt oxide, in aqueous media containing glycine, in order to protect nickel substrate used as cathode of the MCFC. At this stage of the study, and using these conditions, glycine does not allow the formation of more adherent and protective films than without this complexing agent. Nevertheless, a decrease in the glycine concentration could be interesting, allowing to stabilise sufficiently Co(II) in a soluble form without producing a negative effect on the coating adherence. The use of other complexing agents, such as citrates or tartrates, mentioned in the literature, could also be a convenient solution.

Acknowledgment

Dr. Jacques Chivot is gratefully acknowledged for his contribution to thermodynamic predictions.

References

[1] B. Malinowska, M. Cassir, F. Delcorso, J. Devynck, J. Electroanal. Chem. 389 (1995) 21.
[2] M. Cassir, M. Olivry, V. Albin, B. Malinowska, J. Devynck, J. Electroanal. Chem. 452 (1998) 127.
[3] T. Fukui, S. Ohara, T. Tsunooka, J. Power Sources 71 (1998) 239.
[4] T. Fukui, S. Ohara, H. Okwa, T. Hotta, M. Naito, J. Power Sources 86 (2000) 340.
[5] K. Takizawa, A. Hagiwara, J. Electrochem. Soc. 148 (2001) A1032.
[6] L. Mendoza, V. Albin, M. Cassir, A. Galtayries, J. Electroanal. Chem. 548 (2003) 95.
[7] L. Mendoza, R. Baddour-Hadjean, M. Cassir, J.P. Pereira-Ramos, Appl. Surf. Sci. 225 (2004) 356.
[8] T. Pauporté, L. Mendoza, M. Cassir, A. Galtayries, J. Chivot, J. Electrochem. Soc. 152 (2005) C49.
[9] M.J. Escudero, R. Valenzuela, L. Mendoza, M. Cassir, L. Daza, J. Power Sources 140 (2005) 81.
[10] A. Galtayries, L. Mendoza, A. Ringuedé, M. Cassir, J. Electroanal. Chem. 576 (2005) 147.
[11] D. Hem, Roberson, J. Lind, Geochim. Cosmochim. Acta 49 (1985) 801.
[12] M. Dekker, Standard Potentials In Aqueous Solution, New York, 1985.
[13] L. Mendoza, Ph.D. Thesis, ENSCP, University of Paris VI, France, 2003.
[14] B. Malinowska, Ph.D. Thesis, ENSCP, University of Paris VI, France, 1996.
[15] T. Nishina, K. Takiwasa, I. Uchida, J. Electroanal. Chem. 263 (1989) 87.
[16] P. Ganesa, H. Colon, B. Haran, R. White, B. Popov, J. Power Sources 111 (2002) 109.
[17] S.T. Kuk, Y.S. Song, S.I. Suh, J.Y. Kim, K. Kim, J. Mater. Chem. 11 (2001) 630.
[18] S.T. Kuk, Y.S. Song, K. Kim, J. Power Sources 83 (1999) 50.